

Resection of postoperative liver metastasis from pancreatic neuroendocrine tumors: report of one case

Xiao Chen, Hu Ren, Yihebal Chi, Shun He, Zhen Huang, Xuhui Hu, Hong Zhao

Department of Abdominal Surgery, Cancer Institute and Hospital, Chinese Academy of Medical Sciences, Peking Union Medical College, National Cancer Center of China, Beijing 100021, China

Correspondence to: Hong Zhao. Department of Abdominal surgery, Cancer Institute and Hospital, Chinese Academy of Medical Sciences, Peking Union Medical College, National Cancer Center of China, No.17 Panjiayuananli, Beijing 100021, China. Email: pumczhaohong@126.com.

Abstract: Pancreatic neuroendocrine tumor (pNET) is a rare type of pancreatic tumors. The incidence of pNET shows a gradually increasing trend in recent years. Except insulinoma, majority of pNET are metastatic when diagnosis. And liver is the most common organ of distant metastases. Liver metastases are the main determinant for long-term survival and quality of life of patients with pNET. A case of liver metastases of pNET of a 44-year-old female patient is presented in this study. Then we have a brief discussion of the diagnosis and multidisciplinary treatment of advanced pNET.

Keywords: Pancreatic neuroendocrine tumors (pNET); liver metastasis; resection

Received: 18 April 2016; Accepted: 18 April 2016; Published: 01 June 2016.

doi: 10.21037/tgh.2016.05.08

View this article at: <http://dx.doi.org/10.21037/tgh.2016.05.08>

Disease history

A 44-year-old female patient was admitted due to the presence of space-occupying lesions of the pancreas and liver for 1.5 months and over 1 month following surgery for neuroendocrine tumors of the pancreas.

In September 2014, the patient suffered from paroxysmal upper left abdominal pain/discomfort; contrast-enhanced computed tomography (CT) in a local hospital showed the presence of pancreatic mass and hepatic multiple low-density lesions. In October 23, 2014, the patient underwent resection of pancreatic body/tail and spleen in the local hospital. Postoperative pathology showed the presence of neuroendocrine tumors of the pancreas (not reported). The patient did not receive any specific treatment (e.g., medications) after the surgery. During the outpatient visits, the patient did not complain any discomfort and had no paroxysmal hypertension, headache, hyperhidrosis, spontaneous

hypoglycemia, or Whipple's triad. Hepatitis B was diagnosed in October 2014, whereas no other condition was found. Physical examinations did not show any positive sign.

Auxiliary examination

Pathology (November 4, 2014, in our hospital)

Well-differentiated neuroendocrine tumor of the pancreas (4 cm) [WHO grade 2 (G2)] (in distal pancreas and spleen); the tumor had invaded the soft tissue of the pancreas; vascular tumor thrombus and tumor infiltration into nerves were visible; 13 peripancreatic lymph nodes contained metastatic neuroendocrine tumors, whereas no tumor was seen in three lymph nodes (13/16); no tumor was seen in spleen and its resection margin. Immunohistochemistry in other hospital showed chromogranin A (CGA)+, SYN+, and Ki67 =10%.

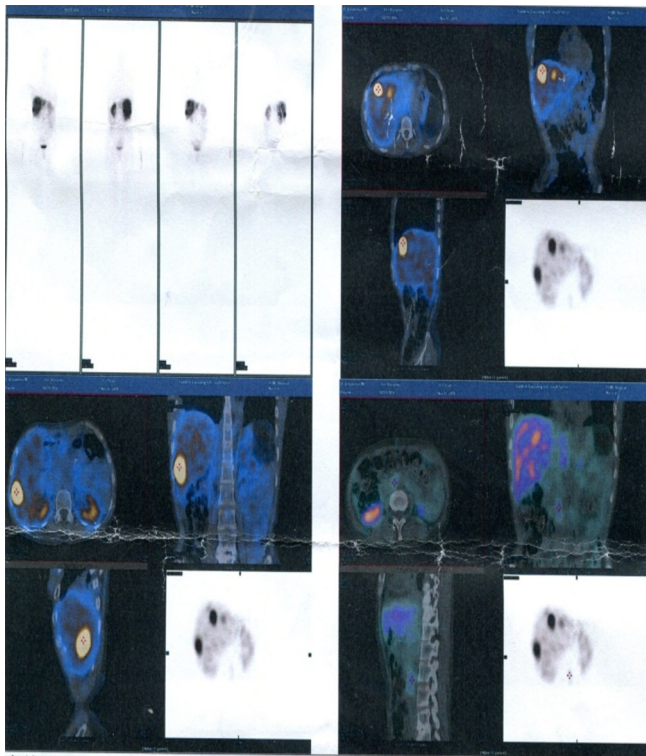


Figure 1 Somatostatin receptor scintigraphy on November 17, 2014.

Somatostatin receptor scintigraphy (SRS) (November 17, 2014, in Peking Union Medical College Hospital)

Multiple sites of abnormally increased radioactive iodine uptake were seen inside liver. Single-photon emission computerized tomography (SPECT)/CT fusion imaging showed multiple areas of abnormally increased radioactive iodine uptake inside liver; a shadow with mildly normally increased radioactive iodine uptake was seen in the neck of pancreas. Initial diagnosis: multiple lesions with high somatostatin expression inside the liver were considered to be metastatic lesions. The lesion with slight somatostatin expression in the neck of pancreas was considered to be a postoperative change (*Figure 1*).

Chest X-ray in our hospital

A nodule-like shadow sized 1.3 cm × 0.8 cm with spiculated margins could be seen near the heart border in the left lower lobe. Light transmission decreased at the costophrenic angle in lower right lung, in which roundish

nodules sized about 1.5 cm × 1.1 cm with relatively regular margin was visible.

Laboratory examinations

CgA 233 ng/mL; routine blood tests, blood biochemistry, and blood coagulation test showed normal results. Tests for hepatitis B virus showed positive results.

Liver magnetic resonance imaging (MRI) (November 26, 2014, in our hospital)

The patient was arranged for a follow-up visit 1 month after the resection of neuroendocrine tumor in the tail of pancreas. Based on the abdominal CT image obtained on October 10, 2014, the MRI finding in current visit were as follows: (I) after the resection of neuroendocrine tumor in the tail of pancreas, the tail of pancreas and the spleen were absent; an oval mass with abnormal signal sized 8.3 cm × 5.2 cm was seen in the spleen area and showed high signal intensity on T1WI; patchy or stripy low-signal-intensity masses were also found, which showed mixed signals on T2WI; in the shadow T1WI showed high signal, which corresponded to restricted diffusion on diffusion-weighted imaging (DWI) sequences in some areas; finally, contrast-enhanced imaging showed border enhancement. Encapsulated pleural effusion was considered. Scattered patchy high-signal mass seen around liver and in the gap between liver and stomach showed high signal intensity on T2WI. Postoperative changes were considered; (II) multiple nodules of various sizes with abnormal signals were seen inside liver sized about 3.3 cm at most. The signals were slightly low on T1WI and high on T2WI, which corresponded to restricted diffusion on DWI sequences. Arterial-phase contrast-enhanced ultrasonography showed margin enhancement, and the enhancement was equal between portal-phase and hepatic parenchyma; the contrast agent was withdrawn in the delayed phase, and no obvious intake was seen in the hepatocyte-specific phase. Multiple metastatic tumors were considered (*Figure 2*).

Chest/abdominal CT plain scans (December 4, 2014, in our hospital)

The abdominal cavity showed postoperative changes. The body/tail of pancreas and the spleen were absent. An oval

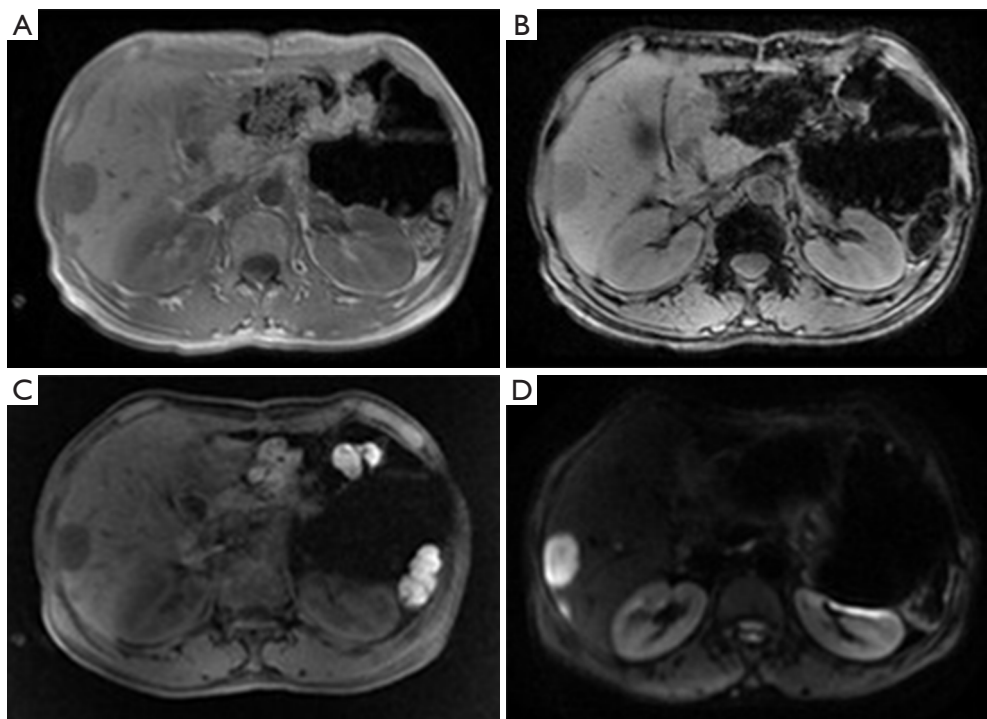


Figure 2 Liver MRI (November 26, 2014).

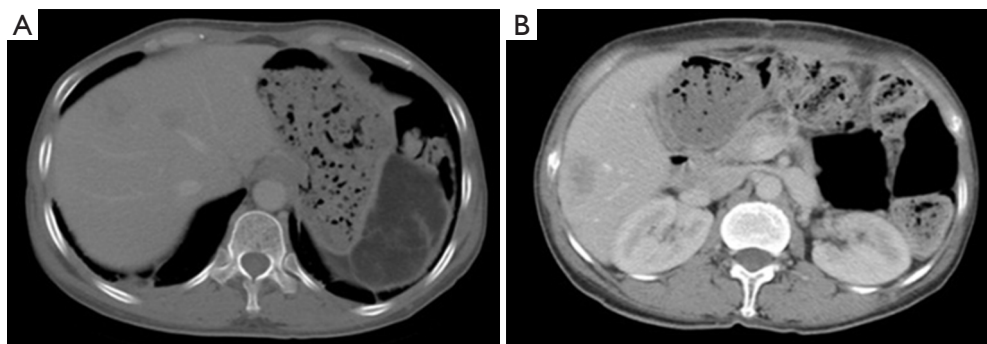


Figure 3 Thoracic and abdominal CT plain scans (December 4, 2014).

low-density mass sized 8.1 cm × 4.8 cm (mainly fat density, inside which there were a few stripy shadows) was seen in the spleen area. Multiple nodules and masses of low densities but with blurred margins were found inside the liver, the larger ones sized about 3.3 cm × 2.1 cm. Multiple metastatic tumors were considered. A small number of patchy or stripy shadows were found in the right lower lobe of the lung and both inferior lobes. These findings were considered to be chronic inflammatory changes, and a close follow-up was recommended. There shows a low-density lesion on thoracic spine, with hardened edge in its margin. A benign tumor was suspected (*Figure 3*).

Surgical treatment

Based on the disease history and the above examination findings, a diagnosis of liver metastases following surgery for neuroendocrine tumors of the pancreas was made; then, resection and radiofrequency ablation of the multiple metastatic tumors were performed under general anesthesia on December 8, 2014. During the surgery, six lesions were surgically removed and three were treated using ultrasound-guided radiofrequency ablation. No ascitic fluid or nodule inside the abdominal and pelvic peritoneum was found during intra-operative exploration. Also, spleen, stomach,

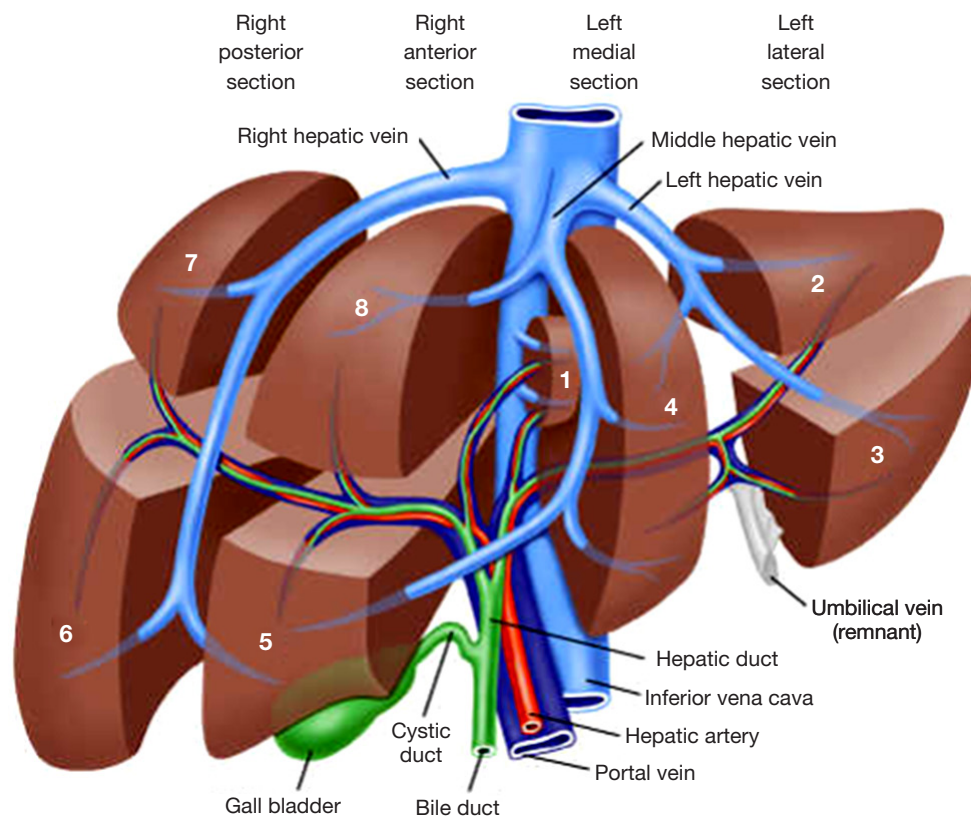


Figure 4 Anatomy of the liver.

small intestine, and large intestine showed no abnormality. The gallbladder and common bile duct were not obviously dilated. The gallbladder had a normal size, and no stone or mass was palpable inside it. No swollen lymph node was palpable near the hepatoduodenal ligament, mesentery, and abdominal aorta. The liver was dark red in color. Combined with findings of intraoperative ultrasonography, totally 12 lesions (all of them were solid masses with well-defined margins): (I) a mass sized about 3.0 cm in segment VI; (II) a nodule sized about 1.0 cm in segment VI; (III) a mass sized about 2.5 cm in segment VIII; (IV) a nodule sized about 1.5 cm in segment VIII; (V) a nodule sized about 0.5 cm in segment V; (VI) a nodule sized about 1.0 cm in the caudate lobe of liver-1; (VII) a nodule sized about 1.0 cm in the caudate lobe of liver-2; (VIII) a mass sized about 0.8 cm in segment VII; (IX) a nodule sized about 0.8 cm in segment II; (X) a nodule sized about 1.0 cm in segment IV; (XI) a nodule sized about 0.8 cm in segment VIII-2; and (XII) a nodule sized about 0.8 cm in segment VIII-3. The falciform ligament, coronary ligament, and left/right triangular ligament of the liver were divided following

the transection and ligation of hepatic round ligament. Exploration was performed as described above after the adhesions were separated. The hepatic hilum was dissected, with a blocking band placed in it. For masses and nodules 1–8, a cutting line was decided about 2 cm away from the tumor margins; then, the liver capsule was cut open using high intensity focused ultrasound (HIFU) and the liver parenchyma was divided using clamping method and electric knife. The piping systems of the liver were sutured or ligated one by one. The lesions were removed en bloc for pathological examination. For nodules 9–12, ultrasound-guided radiofrequency ablation using a single needle was performed; after the ablation, a second intraoperative ultrasound was performed to identify whether the lesions had been completely ablated. After hemostasis was achieved in traumatic liver injury, a second intraoperative ultrasound was performed to identify any untreated lesion. Two drainage tubes were indwelled in liver resection wound and then passed through the right abdominal wall. The surgery was smoothly performed under satisfactory anesthesia. The intraoperative blood

loss was about 200 mL; no blood was transfused (*Figure 4*).

Pathology following resection and radiofrequency ablation for multiple hepatic metastatic tumors (December 9, 2014)

Gross anatomy

(I) Partial liver, sized 7.5 cm × 4.5 cm × 3.5 cm. The liver capsule was partially gray and thickened. There are two nodules inside the cut surface, sizing 3.0 and 1.0 cm respectively. The cut surface was gray-white in color, with neutral nature and relatively clear margin. Its adjacent liver was gray-yellow in color, with neutral nature. The smallest distance between the mass and the basal margin was 0.6 cm; (II) partial liver, sized 6.5 cm × 5.0 cm × 4.0 cm. One nodule was found inside the cut surface, sized 2.5 cm. The cut surface was gray-white in color, with neutral nature and clear margin, involving the liver capsule. The smallest distance between the mass and the basal margin was 0.9 cm; (III) a liver tissue sized 1.2 cm × 1.2 cm × 0.5 cm. One side of the tissue was covered with liver capsule, under which there was a gray-white solid nodule sized 0.3 cm and with clear margin; (IV) partial liver, sized 3.3 cm × 3.5 cm × 2.0 cm. The liver capsule was partially gray-white and thickened. Two nodules, sized 1 cm and 0.9 cm, respectively, were found inside the cut surface. The cut surface was gray-white and gray-yellow in color, with neutral nature and clear margin. The distances between these two nodules and the basal margin were 0.8 cm and 1.1 cm, respectively; (V) a liver tissue sized 4.0 cm × 3.5 cm × 1.7 cm. Dissection from multiple cut surfaces showed the presence of a nodule sized 0.7 cm. It was gray-white in color and had clear margin, but did not involve the capsule. The distance between the nodule and basal margin was 0.4 cm; (VI) partial liver, sized 3.5 cm × 3.9 cm × 2.5 cm. Inside the cut surface there was a mass sized 1.5 cm and close to the basal margin. The cut surface was gray-white in color, with neutral nature and relatively clear margin, and the mass did not involve the liver capsule.

Pathological diagnosis

“Following surgery for neuroendocrine tumors of the pancreas”: (I) mass in segment VI; (II) mass in segment VIII; (III) nodule in segment V; (VI) nodule in caudate lobe of liver; (V) mass in segment VII; and (VI) mass in segment VIII. Liver metastatic neuroendocrine tumors (G2). Mitotic count 3–16/10HPF (mean: 8–10/10HPF). The tumors are multifocal, and vascular tumor thrombi were found. Some tumors involved the liver capsule. No tumor was detected

at the basal resection margin. Infiltration of chronic inflammatory cells was seen in the periportal areas.

Immunohistochemical findings: AE1/AE3 (1+), CK18 (3+), CD56 (3+), Syn (3+), ChrA (2+), Ki-67 (+10%), and hepatocyte (–)

After the surgery, the patient developed hypoproteinemia and pleural fluid, which were improved after nutritional support, inhibiting the secretion of the pancreas, and closed thoracic drainage. The suture was removed from the incision on the 11th postoperative day, and the incision healing was good. The drainage tubes were removed 5 days after their placement. Liver wound drainage tube was withdrawn on the 6th postoperative day and the subphrenic drainage tube was withdrawn on the 8th postoperative day. The patient was discharged on the 11th postoperative day with stable disease condition.

Postoperative treatment

The patient was treated with octreotide for 3 times from December 2014 to February 2015.

Postoperative follow-up

Liver MRI (December 23, 2014, in our hospital)

This follow-up liver MRI was arranged after the resection and radiofrequency ablation of the multiple metastatic tumors following the surgery for pancreatic neuroendocrine tumors (pNET) (the results were compared with the MRI findings on November 26, 2014): (I) the liver had irregular morphology. In the surgical area there were focal effusions, showing high signal on T2WI/FS and low signal on T1WI. In some areas there were fluid–fluid levels (there might be a small amount of bloody fluid), with the range of effusions being 7.0 cm × 4.2 cm and 4.9 cm × 2.7 cm. In the remaining liver parenchyma there were mainly areas showing high signal on T1WI and intermediate or slightly low signal on T2WI/FS. Contrast-enhanced scans showed no abnormal enhancement in the above areas. Thus, these findings were consistent with the changes after surgical treatment and radiofrequency ablation for liver metastatic tumors; (II) there was abnormal DWI signal in the remaining liver parenchyma. The signal was significantly lower in the out-of-phase than in the in-phase on T1WI/dual. Fatty liver was considered; (III) the body/tail of pancreas and the spleen were absent. No definitely abnormal signal or enhanced shadow was seen in the surgical area (*Figure 5*).

Chest/abdominal CT plain scans (January 22, 2015, in our hospital)

The follow-up examination findings were compared with the PACS image obtained on December 4, 2014: the dual lung markings were thick, with scattered small patchy ground-glass opacities. No swollen lymph node was identified in mediastinum. Localized thickening of the pleura was seen in both sides. No pleural or pericardial effusion was found. The abdominal cavity showed postoperative changes. Some structures became altered and disordered, although the anastomosis remained patent. A new low-density area was seen in the original site of liver metastatic tumor and was considered to be a postoperative

change (*Figure 6*).

Thoracic and abdominal CT plain scans (August 4, 2015, in our hospital)

The scans were performed 7 months after the treatment for the metastatic tumor and the findings were compared with those obtained on May 5, 2015: (I) postoperative change of pancreatic tail was absent. No definite abnormality was seen in the local stump, which was similar to the previous finding; (II) no swollen lymph node was identified in abdominal cavity, retroperitoneal area, and mediastinum, and both lungs; (III) multiple irregular low-density areas were seen inside the liver, which was similar to the previous finding. It was considered to a postoperative change. No new metastasis was seen in the liver; (IV) scattered patchy or stripy ground-glass opacities were scattered in both lungs, which were old lesions as found in previous scans; (VI) the spleen is absent. The gallbladder, both kidneys, and bilateral adrenal glands showed no definite abnormality; and (VII) no pleural or pericardial effusion was detected. There was a small amount of effusion around the liver, as found in previous scan (*Figure 7*).



Figure 5 Liver MRI (December 23, 2014).

Discussion

Diagnostic methods of pancreatic neuroendocrine neoplasms (pNENs)

The diagnostic methods of pNENs include qualitative diagnosis and localization.

The qualitative diagnosis means the identification of a specific lesion, during which needle biopsy is a commonly used procedure. For resectable pancreatic tumors, however, preoperative pathology is not required. The common serological markers of pNENs include CgA and neuron-

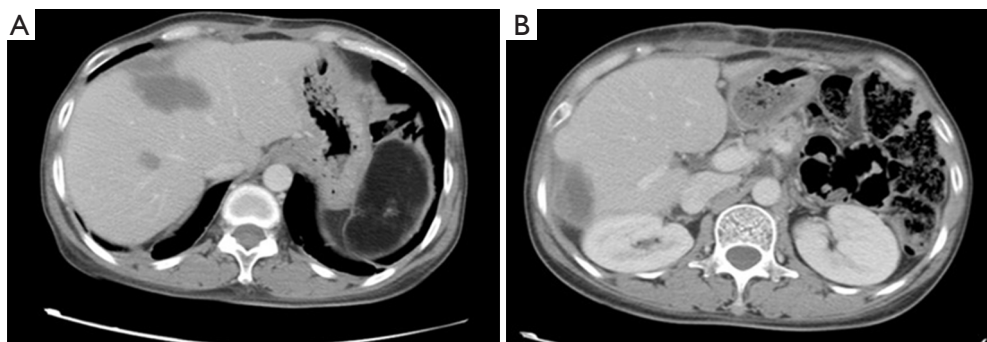


Figure 6 Thoracic and abdominal CT plain scans (February 22, 2015).

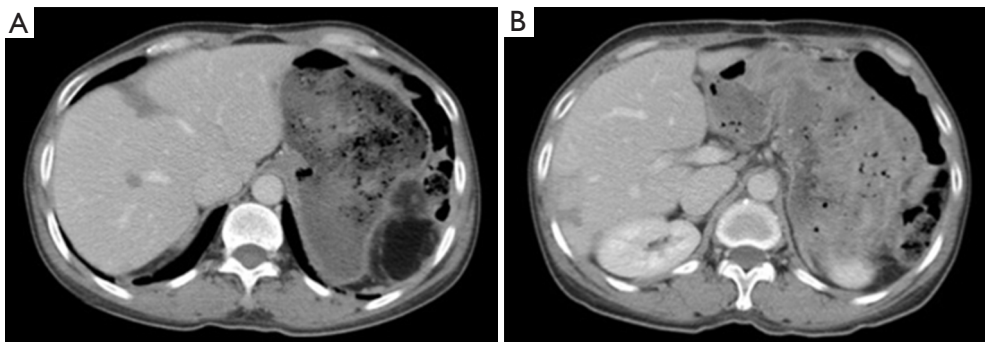


Figure 7 Thoracic and abdominal CT plain scans (August 4, 2015).

specific enolase (NSE), whose abnormal increase often indicates the possibility of a neuroendocrine tumor. For functional pNENs, the hormone secretion-related symptoms and serum hormone levels can be used to judge the functional status of a specific tumor and inform the symptomatic treatment of hormone-related symptoms (1).

Localization is a key step in the surgical treatment for pNENs. Localization can identify the site of a primary tumor and meanwhile help to assess the status of lymph nodes around the tumor and the presence of any distant metastasis. The localization can be roughly divided into two categories: (I) non-invasive examinations including ultrasound, spiral CT three-dimensional reconstruction, vascular perfusion imaging, endoscopic ultrasound (EUS), MRI, PET-CT, SRS, and intraoperative ultrasonography; and (II) invasive approaches including selective arterial angiography, arterial stimulation venous sampling (ASVS), and percutaneous transhepatic portal catheterization (PTPC). These invasive examinations are the mainstream approaches for localization in the 20th century, and the sensitivities of angiography, ASVS, and PTPC reached 70%, 94%, and 88%, respectively. However, these examinations are complicated, painful and time-consuming; meanwhile, they can be accompanied by certain surgical risks. Along with the introduction of non-invasive techniques, these examinations have gradually phased out both in China and abroad. They may be used only in patients with highly suspicious PET-CT but with negative results after all non-invasive examinations. Multidetector spiral CT is currently the preferred method for clinical localization. Using its three-dimensional reconstruction technique, it can clearly display the relationships between a tumor and its surrounding vessels, pancreatic duct, and bile duct, thus informing the selection of a surgical procedure. Foreign literature has reported that it has a diagnostic sensitivity of 85–100% for

insulinoma; in China, its diagnostic positive rate for PET-CT also reached 80% or higher. SRS has been rapidly evolving in recent years. EUS has been widely used in the past years. In Chinese literature, EUS has a diagnostic positive rate of about 90% for PET; meanwhile, for PET that can not be detected by abdominal ultrasound and CT, EUS also can achieve a detection rate of 80%. Thus, it can supplement these two examinations and vice versa. However, EUS is less sensitive for diseases located at the tail of pancreas, with a sensitivity of only around 40%. It has been described in a foreign literature that EUS-guided fine-needle puncture for injecting India ink might achieve the rapid intraoperative localization of tumors in patients with small tumors that were difficult to locate during surgery (2).

Multidisciplinary treatment of pNENs

Surgical treatment of the liver metastasis of pNENs

Liver is the most common site for pNENs metastasis. If surgery can remove most (>90% of lesions) metastases, concurrent or staged resection of the primary lesion and liver metastases may be considered. If the tumor is located in the head of the pancreas, it is recommended that resection of liver metastasis should be performed firstly before the removal of pancreas and duodenum by a second surgery. Resection of liver metastases should meet the following conditions: (I) well-differentiated G1/G2 tumors; (II) without distant lymph node metastasis, extrahepatic metastasis, or diffuse peritoneal metastasis; and c) without right cardiac dysfunction. The 5-year survival rate following the resection of liver metastases ranges 47–76%, which is higher than those (30–40%) in non-resected patients; however, the recurrence rate can reach 76% after the resection and the recurrence mostly occurs within 2 years. Local treatments including radiofrequency ablation, arterial chemoembolization, and selective internal

radiotherapy can control the liver metastasis, lower tumor burden, reduce hormone secretion, and thereby improve the patient's quality of life. Currently no prospective clinical trial has demonstrated that a local treatment targeting the liver may improve the prognosis of patients; however, these local treatments are often used in combination with systemic treatment in clinical settings; (III) liver transplantation: Liver transplantation has been used for the treatment of the liver metastasis of pNENs; however, its surgical indications must be strictly followed. The indications of liver transplantation are as follows: the pNENs are accompanied by unresectable multiple liver metastases but without extrahepatic metastasis or regional lymph node metastasis; the primary lesion can be completely resected, and biopsy shows the fraction of Ki-67-positive tumor cells is <10% (Ki-67<5% means better prognosis); with symptoms that can not be medically controlled and severely affect the patient's quality of life; and without any contraindication of liver transplantation.

Drug therapy of metastatic pNENs

(I) Somatostatins: somatostatins has an objective response rate of <10% for pNENs; however, it can achieve a disease control rate of up to 50–60%. As shown in many retrospective studies and randomized prospective studies, somatostatins can be used in patients with slowly progressing pNENs (G1/G2) and somatostatin receptor-positive pNEC (G3), with relatively mild adverse reactions; (II) molecularly targeted drugs: prospective clinical studies have demonstrated that sunitinib and everolimus have good efficacy for advanced and metastatic pNENs and can be well tolerated by patients. Sunitinib is a multitargeted receptor tyrosine kinase inhibitor and everolimus is an orally administered mTOR inhibitor. Both of them can significantly prolong the progression-free survival in pNEN patients; (III) chemotherapy: the role of streptozotocin combined with 5-fluorouracil (5-FU) and (or) epirubicin in treating G1/G2 pNENs has been well demonstrated, with an objective response rate of 35–40%. A recent retrospective study with small sample size indicated that temozolomide monotherapy or in combination with capecitabine also has a certain efficacy in treating metastatic pNENs. 5-FU or capecitabine combined with oxaliplatin or irinotecan can also be used as the second-line treatment options for pNENs.

Postoperative adjuvant therapy

Up to now no high-quality evidence has supported the application of adjuvant therapies such as long-acting somatostatins, chemotherapy, or molecularly targeted drugs

might benefit pNENs patients following R0/R1 resection. Thus, adjuvant therapies should not be routinely used in G1/G2 pNENs patients following radical resection. However, clinical research on the adjuvant therapies can be considered in patients at high risk of tumor relapse (e.g., lymph node metastases, intravascular thrombi, and/or positive margin). In patients with pathologically confirmed G3 pNENs following radical treatment, systemic adjuvant therapies and/or local treatment may be applied in accordance with the principles of treatment for ductal adenocarcinoma. In patients with both primary and metastatic pNENs, adjuvant therapy may be provided following the R0 resection of primary and metastatic lesions to prevent relapse. However, there is no widely recognized protocol for this condition, and prospective clinical studies are warranted (1).

Acknowledgements

None.

Footnote

Conflicts of Interest: The authors have no conflicts of interest to declare.

Informed Consent: Written informed consent was obtained from the patient for publication of this case report and any accompanying images. A copy of the written consent is available for review by the Editor-in-Chief of this journal.

References

1. Pancreatic Surgery Group of Surgery Branch of Chinese Medical Association. Guidelines for the diagnosis and treatment of Pancreatic Neuroendocrine Neoplasms (2014 edition). Chinese Journal of Practical Surgery 2014;34:1117-9.
2. Zhao Y. The current status and disparity in diagnosis and treatment of pancreatic endocrine tumor in China. Chinese Journal of Practical Surgery 2010;30:729-32.

doi: 10.21037/tgh.2016.05.08

Cite this article as: Chen X, Ren H, Chi Y, He S, Huang Z, Hu X, Zhao H. Resection of postoperative liver metastasis from pancreatic neuroendocrine tumors: report of one case. *Transl Gastroenterol Hepatol* 2016;1:47.